Advanced Physical Research
Vol.5, No.3, 2023, pp.133-145

# EPOXY-W COMPOSITE MATERIALS: MICROSTRUCTURE, STRUCTURE, AND RADIATION EFFICIENCY

**A.A. Rotkovich[1*], D.I. Tishkevich[1], A.A. Bondaruk[1], S.A. German[1,2], I.U. Razanau[1], T.I. Zubar[1], E.S. Dashkevich[1], Y.I. Aliyev[3], S.V. Leonchik[1], S.V. Trukhanov[1], A.V. Trukhanov[1]**

[1]SSPA «Scientific-Practical Materials Research Centre of NAS of Belarus», Minsk, Belarus
[2]Belarusian National Technical University, Minsk, Belarus
[3]Azerbaijan State Pedagogical University, Baku, Azerbaijan

**Abstract.** Composite materials based on epoxy resin and tungsten (W) with varying content from 0 to 80% using the chemical curing method were obtained. For samples with content up to 40%, agglomeration of W grains have been revealed. Statistical analysis of W grain sizes demonstrated that their probable diameter size is 475 nm. The effective density varied with the W powder content, and the relative density was between 91% and 94%, indicating that there were no significant defects. The X-ray diffraction analysis showed the presence of the main bulk-centered cubic W and $WO_2$ phases, indicating the oxidation of W in the surface layer of the material. Calculating in Phy-X/PSD software allowed to evaluate the gamma radiation shielding efficiency for composite materials. Samples with 60 and 80% W content were found to be the most suitable candidates for radiation shielding application. It was found that the addition of W powder to the epoxy matrix leads to a 3.5 times decrease in the values of the half-value layer at a gamma-ray energy of 1.25 MeV. The obtained results show the high efficiency of the proposed composite materials in gamma shielding, which makes them suitable for creating radiation shields.

***Keywords:*** *Tungsten, epoxy resin, polymer, radiation shielding, gamma-ray.*

***Corresponding Author:*** *A.A. Rotkovich, SSPA «Scientific-Practical Materials Research Centre of NAS of Belarus», 220072, Minsk, Belarus, Tel.: 8(017)367-00-26, e-mail: rottkovich@gmail.com*

***Received:*** *07 June 2023;* ***Accepted:*** *22 July 2023;* ***Published:*** *03 October 2023.*

## 1. Introduction

Ionizing radiation destroys molecules and molecular bonds, leading to changes in the chemical structure of compounds. It encompasses photon radiation, including X-rays and gamma-rays (Hou *et al.*, 2017; Li *et al.*, 2017). This type of radiation has a negative impact on human life activity and the environment (Sahin *et al.*, 2021), so the research in the field of radiation shielding is very relevant. When gamma-quanta interact with electrons and cores of substances, photo- and Compton effects, the effect of birth of electron-positron pairs arise. Radiation shields containing such high-density materials as lead and concrete are used to protect people and equipment from high-energy gamma radiation (Sayyed *et al.*, 2021b; Tishkevich *et al.*, 2020a; Tishkevich *et al.*, 2020b; Vorobjova *et al.*, 2019). However, these materials have high mass-dimensional

**How to cite (APA):**
Rotkovich, A.A., Tishkevich, D.I., Bondaruk, A.A., German, S.A., Razanau, I.U., Zubar, …, & Trukhanov, A.V. (2023). Epoxy-W composite materials: Microstructure, structure, and radiation efficiency. *Advanced Physical Research, 5*(3), 133-145.

characteristics, and lead has a serious disadvantage – significant toxicity (Wani *et al.*, 2015). As a consequence, great attention is paid to the development of new lightweight materials with good radiation shielding parameters. Such materials are used in various industries such as medicine (Abualroos *et al.*, 2019), electronics (Thibeault *et al.*, 2015), aerospace (Pitchan *et al.*, 2017) and nuclear (Kim *et al.*, 2014) industries.

Many studies have been conducted on radiation-polymer topics covering both thermoplastic and thermosetting polymers. Materials such as plastics and resins have low density and are lightweight (Banerjee *et al.*, 2019; Prabhu *et al.*, 2021; Muthamma *et al.*, 2019; Almurayshid *et al.*, 2021; Shang *et al.*, 2020; İrim *et al.*, 2018; Trukhanov *et al.*, 2022). Polymeric materials are also characterized by easy processing, durability, chemical and corrosion resistance and good adhesion properties (Lozitsky *et al.*, 2020; Saba *et al.*, 2015; Shin *et al.*, 2014; Rohini *et al.*, 2019; Alavian *et al.*, 2020; Saleem *et al.*, 2021; Saiyad *et al.*, 2021). Matrices based on epoxy resin, polyethylene, silicone and polyimide have been actively studied by the scientific community (Aldhuhaibat *et al.*, 2021; Alavian *et al.*, 2019; Yılmaz *et al.*, 2021; Pavlenko *et al.*, 2019). Composite materials with epoxy matrix and 30% $WO_3$ and $HfO_2$ particles were synthesized (Higgins *et al.*, 2019). The experimental results showed that when the samples with $WO_3$ and $HfO_2$ were irradiated with 356 KeV energy, the mass attenuation coefficient was only 0.128 and 0.129 $cm^2/g$, respectively. Although tungsten and hafnium are considered high-density materials, but due to their small content, the degree of protection against ionizing radiation is limited due to the low density of the samples. In general, epoxy resin composites are well established for radiation shielding due to its excellent thermal stability and long-term radiation resistance (Hou *et al.*, 2017). Moreover, epoxy resin is a low-cost and quite common material (Yu *et al.*, 2021). All these advantages makes epoxy matrix composites promising materials for their use as radiation shields.

Composites with fillers such as Bi, W-containing compounds, ZnO, CdO, etc. have been repeatedly used for the development of shielding materials (El-Fiki *et al.*, 2015; Elsafi *et al.*, 2023; Alsayed *et al.*, 2020; El-Khatib *et al.*, 2019; Tishkevich *et al.*, 2022; Tishkevich *et al.*, 2019; Dong *et al.*, 2022; Kozlovskiy *et al.*, 2019; Tishkevich *et al.*, 2018 a; Tishkevich *et al.*, 2018 b). Also, in the literature one can find information about materials for protection against neutron and gamma radiation simultaneously. These are mainly multilayer materials or materials containing $B_4C$ or $B_2O_3$, BN (Castley *et al.*, 2019; Araz *et al.*, 2021; Li *et al.*, 2019). In contrast, materials based on carbon fiber, fabrics are not so effective due to the presence of elements with low atomic number (Z) (Wu *et al.*, 2013; Sayyed *et al.*, 2016). Epoxy composites with $Bi_2O_3$ and $WO_3$ (content up to 30%) were studied for resistance to gamma radiation (Karabul *et al.*, 2021). The half-value layer (HVL) for samples with $Bi_2O_3$ and $WO_3$ (30%) at irradiation energies of 81-1332 KeV was 0.666-9.160 cm and 0.237-8.156 cm, respectively. At low energies, the thickness of the sample with $WO_3$ is found to be almost 3 times smaller than that for the sample with $Bi_2O_3$, making it a more suitable candidate for radiation shielding material. A study-comparison of $Bi_2O_3$ and $WO_3$ fillers with PbO in terms of shielding ability and the effect of micro- and nano-particles on the value of mass attenuation coefficient (MAC) was performed (Verdipoor *et al.*, 2018). The study confirmed that using nano-sized $Bi_2O_3$, $WO_3$ and PbO particles (50% content) at an energy of 0.3559 MeV, the MAC increases slightly compared to micro particles and is 0.1099, 0.1097, 0.1098 $cm^2/g$, respectively. The values for samples with $Bi_2O_3$ and $WO_3$ components are similar to PbO, which proves the possibility of lead-free materials.

Recently, mathematical modeling methods have become popular. The main software packages used for modeling the attenuation processes of the investigated materials are WinXCOM (Sayyed *et al.*, 2022; Sayyed *et al.*, 2021a) GEANT4 (Abbas *et al.*, 2021; Canel *et al.*, 2019) and Phy-X/PSD (Şakar *et al.*, 2020; Singh *et al.*, 2020; Lacomme *et al.*, 2021), as well as the Monte Carlo method (MCNPX) (Afaneh *et al.*, 2022; Khattari *et al.*, 2022; Liu *et al.*, 2022). In the analysis of the glass system, a comparative study between the results of attenuation of high-energy particle flux by experiment and simulation in WinXCOM (Sayyed *et al.*, 2022) was carried out. It was found that the results were in good agreement with each other. A study of glass system with $WO_3$ particles was discovered (Singh *et al.*, 2020). Gamma-ray shielding results are derived by simulation methods in Phy-X/PSD and WinXCOM software. As a result, in the energy range of 0.015-15 MeV, the percentage of deviation between the measurements of the two programs was not more than 1.5. All this indicates that the modeling methods are accurate and reliable, and give prospects for their use in planning the experiment.

The aim of the work is to study the microstructure, chemical and phase composition, density values and gamma radiation shielding efficiency parameters of epoxy resin-W composite materials.

## 2. Materials and Methods

Composite materials were obtained from ED-20 epoxy resin and tungsten powder of analytical purity with addition of polyethylene polyamine (PEPA) hardener. The mass content of tungsten was varied from 0 to 80% with steps of 20%. The experimental samples were coded according to the cipher given in Table 1.

**Table 1.** Code names of composite materials of epoxy-W system

| Code name | Epoxy resin content, % | Tungsten content, % |
|---|---|---|
| EP100 | 100 | 0 |
| EP80W20 | 80 | 20 |
| EP60W40 | 60 | 40 |
| EP40W60 | 40 | 60 |
| EP20W80 | 20 | 80 |

A schematic representation of the experimental methodology is presented in Fig.1.

Epoxy resin and W powder were weighed in stoichiometric ratios and mixed on a magnetic stirrer for 15 min (Fig. 1 A). The materials were then transferred to a water bath heated to 50°C to release air bubbles and obtain a more homogeneous composite structure (Fig. 1 B). After the composites cooled, hardener was added in an amount of 10% of the resin mass content and the samples were homogenized for 10 minutes (Fig. 1 C). After this, the composites were poured into silicone molds with cell sizes of 4.8x4.8 $cm^2$ (Fig. 1. D). The curing of the materials took place over 24 h. Post-synthesis processing of the experimental samples was carried out using a FORCIPOL 202 grinding and polishing machine to obtain uniform and planar samples with a thickness of 1 mm (Fig. 1 E).

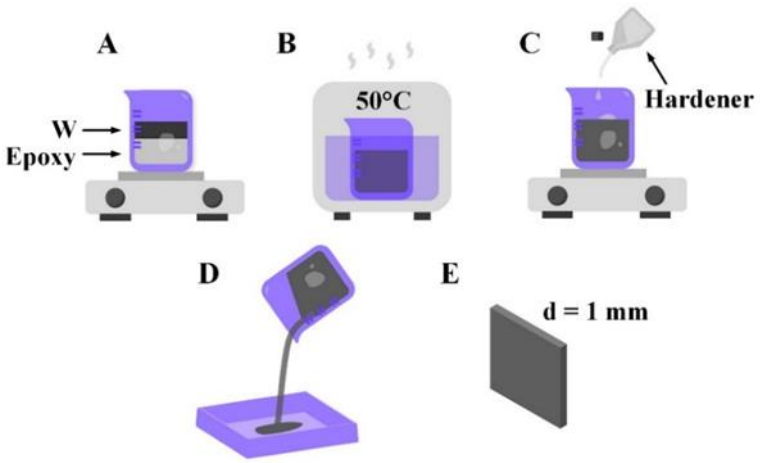


**Fig. 1.** Methodology of manufacturing of epoxy resin-W composite materials

The morphology and chemical composition of the obtained composites were studied using a Carl Ziess EVO10 scanning electron microscope (SEM) and an Oxford attachment for energy dispersive X-ray spectroscopy. The raw data for the statistical analysis of W grain size distribution conducted using SmartSEM software were collected from at least three SEM images. Phase analysis and structure of the epoxy resin-W composites were carried out by X-ray diffraction method on a POWDIX 600/300 diffractometer. The measurements were carried out in the range 2Θ = 5-140° with a step of 0.05°. The effective density of the samples was measured according to the Archimedes method (Crawley *et al.*, 1974).

$$\rho = \frac{M}{M-m} \cdot \rho_{H_2O}, \quad (1)$$

where M is the mass of the sample in air, g; m - mass of the sample in liquid, g; $\rho_{H2O}$ - density of water, g/cm$^3$.

The above formula was used to determine the theoretical density:

$$\rho_{theor} = \frac{1}{V}, \quad (2)$$

where V is the volume of the composite mixture, which is defined by the formula:

$$V = \frac{\omega_{epoxy}}{\rho_{epoxy}} + \frac{\omega_W}{\rho_W}, \quad (3)$$

where $\omega_{epoxy}$ - mass content of epoxy resin expressed in fractions; $\omega_W$ - mass content of tungsten; $\rho_{epoxy}$ - table value of epoxy resin density, g/cm$^3$; $\rho_W$ - table value of tungsten density, g/cm$^3$.

Relative density shows how many percent the density of the experimental sample (effective density) is close to the reference density value (theoretical density). As the effective density we take the density calculated by the Archimedes method.

Relative density was calculated by the formula:

$$\rho_{rel} = \frac{\rho_{ef}}{\rho_{theor}} \cdot 100\%, \quad (4)$$

where $\rho_{ef}$ – effective density, g/cm$^3$; $\rho_{theor}$ – theoretical density, g/cm$^3$.

The presence of porosity may be due to the peculiarity of the purpose of the obtained material. However, in our case porosity negatively affects the microstructure, worsening the necessary properties of the material (density).

The porosity was measured as follows:

$$P = 100\% - \rho_{rel}, \quad (5)$$

The gamma-ray shielding efficiency parameters were calculated in Phy-X/PSD software for the linear attenuation coefficient (LAC), half-value layer (HVL), and mean free path (MFP). The above calculations were performed in the energy range of 0.8-2.5 MeV for the $^{60}$Co source.

When gamma radiation interacts with matter, photo-, Compton effects and the birth of electron-positron pairs occur. The greater the effect of these effects, the more effective is the attenuation of radiation. The synergetic action of the effects is characterized by the LAC of gamma-quanta. The LAC shows the relative decrease of flux density per unit thickness of a substance and is determined by the formula:

$$LAC = \ln\left(\frac{I/I_0}{x}\right), \quad (6)$$

where $I$ is the intensity of falling radiation; $I_0$ - intensity of the passed radiation; x - material thickness, cm.

The HVL defines the thickness of matter required to shield the radiation by half:

$$HVL = \frac{0{,}693}{LAC}, \quad (7)$$

The MFP describes the distance a gamma-ray quantum traverses without collisions. However, the greater the number of collisions, the more effectively the radiation flux is shielded. Also, this quantity is the inverse of the LAC:

$$MFP = \frac{1}{LAC}. \quad (8)$$

## 3. Results and Discussion

Fig. 2 shows the SEM image of the initial W powder (A) as well as the W grains distribution diagram (B).

In order to determine the most probable W grain size, the Gaussian function was used to approximate the distribution curve. It is shown that the most probable diameter of W grain size is 475 nm.

The results of the SEM study of the cross section of the composites are summarized in Fig. 3.

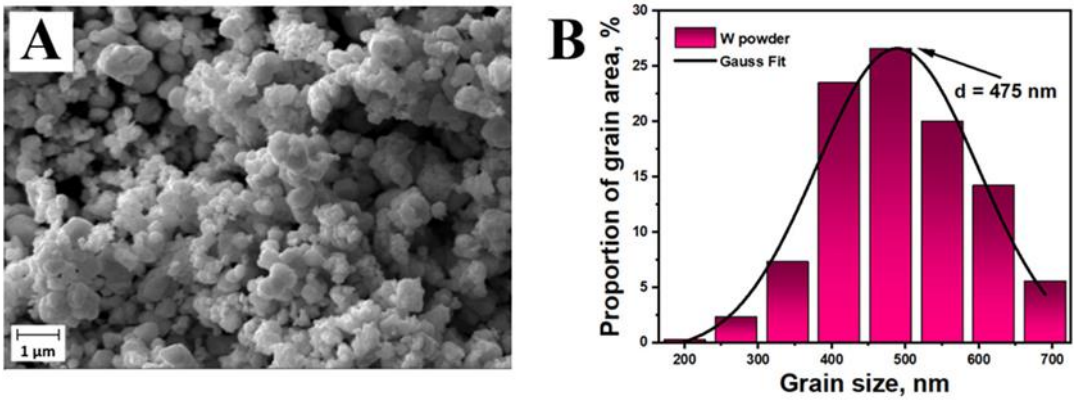


**Fig. 2.** Grain distribution of the W powder: (A) initial SEM image; (B) distribution diagram

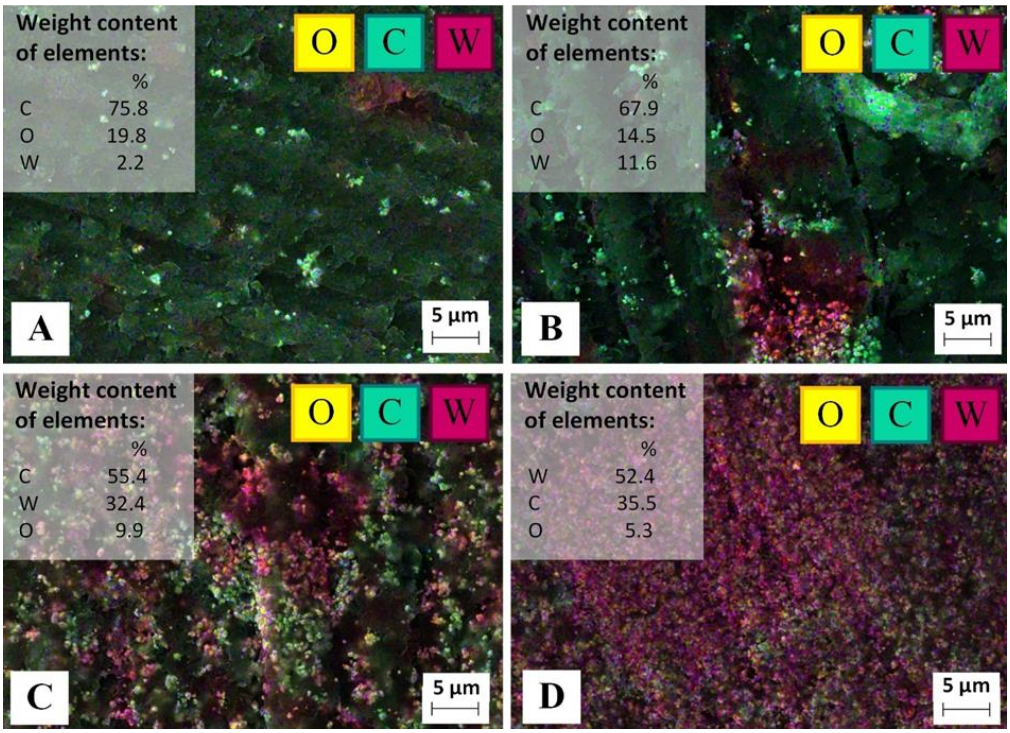


**Fig. 3.** SEM images of epoxy resin-W composite materials: (A) sample EP80W20; (B) sample EP60W40; (C) sample EP40W60; (D) sample EP20W80. Inserts: Weight content of elements

It can be seen from the results that the W grains are surrounded by a polymer matrix. In particular, in Fig. 3 (A) and (B), rare clusters of agglomerated groups of W powder are clearly visible. However, it is observed that as the filler content increases up to 60 and 80% (Fig. 3, C, D), a more homogeneous distribution of W powder is noticed. The grains are visually visible throughout the entire volume of the matrix, there are practically no areas in the sample with voids and pores. This is also confirmed by the results of chemical composition distribution, presented in the inserts. The studied samples contain W and polymeric component represented by C and O. Also, the weight contents of each element in percentages are given in the images. The quantitative composition of W varies from 2.2 to 52.4%.

In general, taking into account the results of SEM analysis only, it can be stated that the samples EP40W60 (Fig. 3, C) and EP20W80 (Fig. 3, D) are most suitable for the purposes of the study due to the homogeneous distribution of the filler.

The results of X-ray diffraction analysis are presented in Fig. 4.

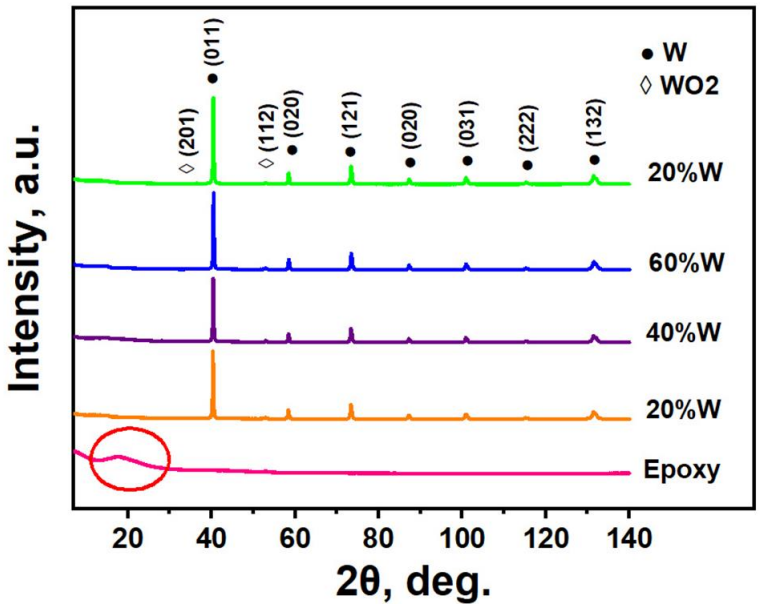


**Fig. 4.** Results of X-ray diffraction analysis of epoxy resin-W composite materials

It can be observed that the epoxy resin-W composite system consists of two phases: W phase and tungsten oxide phase $WO_2$ (Fig. 4). It should be noted that tungsten oxidizes at 415 °C, which means that the X-ray diffraction analysis should not have revealed the oxide phase, since the samples were fabricated at temperatures below 50 °C during the synthesis process. The presence of the oxide phase can only be explained by a surface phenomenon, which is the oxidation process of the thin surface layer of the initial powder even at room temperature. In the diffractogram characteristic of pure epoxy resin, an amorphous halo can be seen (highlighted with a red circle), as expected when analyzing amorphous substances.

Table 2 presents the values of effective density of epoxy resin-W composite materials.

**Table 2.** Values of the effective density of epoxy resin-W composite materials

| Code name | Effective density, g/cm$^3$ |
|---|---|
| EP100 | 1,16 |
| EP80W20 | 1,40 |
| EP60W40 | 1,75 |
| EP40W60 | 2,56 |
| EP20W80 | 4,36 |

It was observed that with the increase of W powder content from 0 to 80% there is an enlargement of effective density from 1.16 to 4.36 g/cm$^3$. Calculation of relative densities showed that their values vary in the range of 91-94% (Fig. 5).

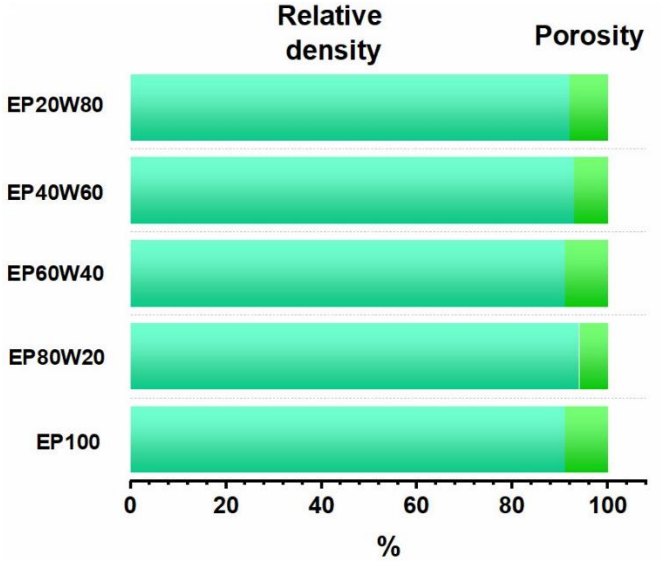


**Fig. 5.** Dependence of the relative density and porosity of epoxy resin-W composite materials on the percentage of filler content

It can be observed that for all samples it is characteristic that all values are above 90%, which allows us to conclude a high degree of homogenization of the samples and insignificant porosity. The porosity values for all the experimental samples are almost at the same level and do not exceed 10%. Consequently, raising the content of W powder in the system from 0 to 80% did not significantly affect the formation of defects and pores.

Fig. 6 shows the results of calculations in the Phy-X program of the main parameters describing the shielding efficiency of gamma radiation. As noted earlier, the larger the LAC values, the higher the shielding efficiency. It can be observed that with the increase of radiation energy from 0.8 to 2.5 MeV the LAC values reduce and the shielding properties of the investigated samples epoxy-W after the action of 1.25 MeV energy significantly weaken (Fig. 6, A). For example, the LAC of the EP20W80 sample at radiation energies of 0.8 and 1.25 MeV has values of 0.340 and 0.235 $cm^{-1}$, respectively, which is almost 31% less.

It can be concluded from the graph that the sample with 80% filler content has the highest LAC values compared to the rest of the samples.

The same can be said about the results of HVL calculating (Fig. 6, B). The composite materials have a relatively low density, whereas higher energy attenuation requires samples with higher thickness. Thus, the presented materials are recommended to be used at gamma-ray energies up to 1.25 MeV, since further with increasing radiation energy there is a strong build-up of the thickness of the samples.

However, the addition of W powder to the system up to 80% contributed to a substantial decrease in HVL parameter. For comparison, the values of HVL at gamma-ray energy of 1.25 MeV for pure epoxy resin samples and those with maximum W content are 9.488 and 2.672 cm, accordingly. In this regard, it is observed that there was a 3.5 times reduction in the HVL values of the samples.

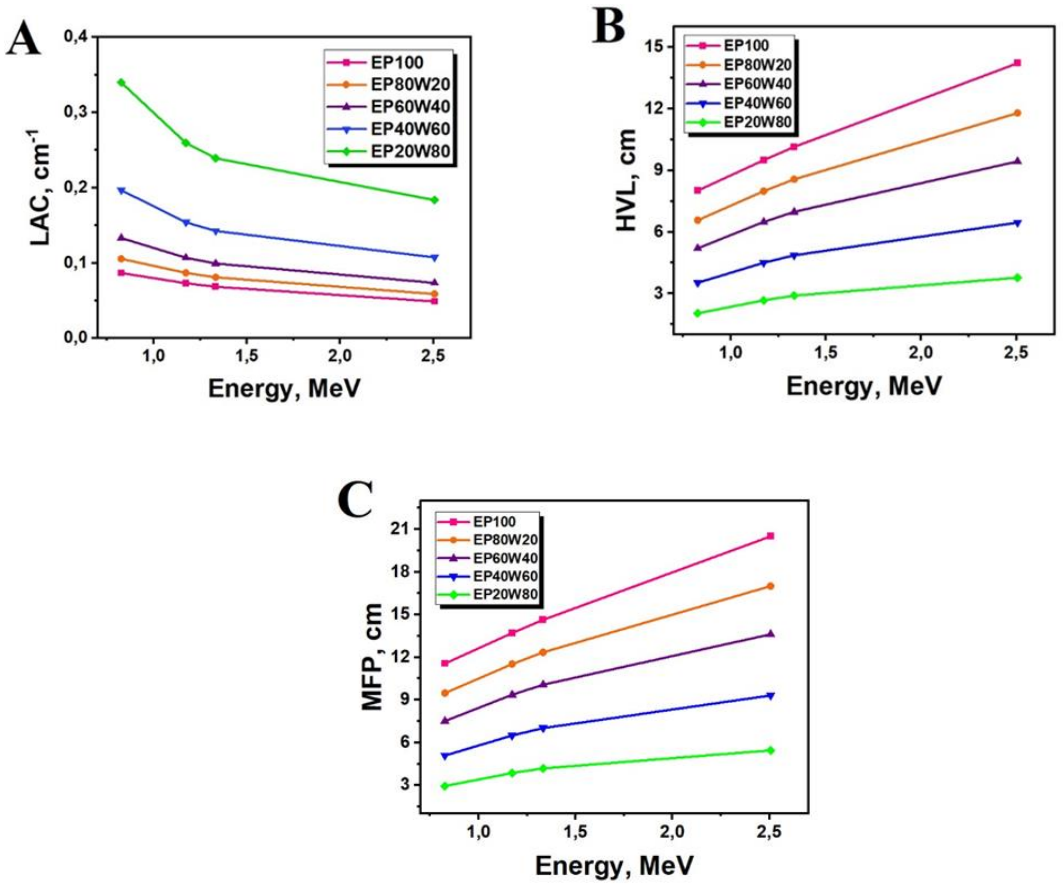


**Fig. 6.** Graphs of dependence of linear attenuation coefficient (A), half-value layer (B) and mean free path (C) on gamma radiation energy of epoxy resin-W composite materials.

It is showed that the results of calculating of MFP (Fig. 6, B), correlate with the results of calculation of HVL. Also, it can be said that in the system of composite materials epoxy resin-W sample EP20W80 stands out by its shielding characteristics, having significantly lower values of MFP. In particular, the maximum values of MFP for EP100 and EP20W80 samples are 20.512 and 5.449 cm, simultaneously.

Thus, it can be deduced that composite materials with W filling of 80% and more are more appropriate for creation of radiation shields due to their high shielding properties and improved mass-dimensional parameters.

## 4. Conclusion

Composite materials of epoxy resin-W system with different filler content from 0 to 80% were obtained by chemical curing method. The microstructure of the cross-section of the samples was investigated by scanning electron microscopy, which showed that with increasing mass fraction of filler there is a more homogeneous distribution of W grains in the epoxy matrix. The occurrence of agglomerates of W grains was noted for samples with filler up to 40%.

A statistical analysis of W grain sizes was carried out, which showed that the most probable W grain size is 475 nm. The values of effective density of experimental samples were obtained by experimental method and the values of relative density were determined by calculation. With increasing W powder content, the effective density changes from

1.14 to 4.36 g/cm$^3$ for the epoxy-W system. The relative density varies between and 91-94% indicating the least defect free test.

The crystalline structure of the composites was evaluated using X-ray diffraction analysis. Also, the analysis revealed the presence of the main bulk-centered cubic W and $WO_2$ phases for the two systems studied. The diffractogram corresponding to the pure epoxy resin shows characteristic broadband peaks.

Based on the results of calculation the shielding efficiency from ionizing radiation in Phy-X/PSD software, the values of such parameters as LAC, HVL, and MFP were obtained. The samples EP40W60 and EP20W80 are most suitable for radiation shielding. For complete absorption of 1.25 MeV energy, EP20W80 samples with a thickness of 2.672 cm would be required, and to shield the same amount of energy, an EP100 sample would need to be 9.448 cm thick. The results of the study prove the possibility of using composites as shielding materials against gamma radiation, due to their different values of shielding efficiency parameters.

## References


Abbas, M.I., Alzahrani, J.S., Sayyed, M.I., Tishkevich, D.I., Alabsy, M.T., El-Khatib, A.M. & Elsafi, M. (2021). Gamma-Ray Attenuation and Exposure Buildup Factor of Novel Polymers in Shielding Using Geant4 Simulation. *Materials*, 14, 5051.

Abualroos, N.J., Amin, N.A.B. & Zainon R. (2019). Conventional and new lead-free radiation shielding materials for radiation protection in nuclear medicine: A review. *Radiation Physics and Chemistry*, 165, 108439.

Afaneh, F., Khattari, Z.Y. & Al-Buriahi, M.S. (2022). Monte Carlo simulations and phy-X/PSD study of radiation shielding and elastic effects of molybdenum and tungsten in phosphate glasses. *Journal of Materials Research and Technology*, 19, 3788-3802.

Alavian, H., Tavakoli-Anbaran, H. (2019). Study on gamma shielding polymer composites reinforced with different sizes and proportions of tungsten particles using MCNP code. *Progress in Nuclear Energy*, 115, 91-98.

Alavian, H., Samie, A. & Tavakoli-Anbaran, H. (2020). Experimental and Monte Carlo investigations of gamma ray transmission and buildup factors for inorganic nanoparticle/epoxy composites. *Radiation Physics and Chemistry*, 174, 108960.

Aldhuhaibat, M.J.R., Amana, M.S., Jubier, N.J. & Salim, A.A. (2021). Improved gamma radiation shielding traits of epoxy composites: Evaluation of mass attenuation coefficient, effective atomic and electron number. *Radiation Physics and Chemistry*, 179, 109183.

Almurayshid, M., Alsagabi, S., Alssalim, Y., Alotaibi, Z. & Almsalam, R. (2021). Feasibility of polymer-based composite materials as radiation shield. *Radiation Physics and Chemistry*, 183, 109425.

Alsayed, Z., Badawi, M.S., Awad, R., El-Khatib, A.M. & Thabet, A.A. (2020). Investigation of $\gamma$-ray attenuation coefficients, effective atomic number and electron density for ZnO/HDPE composite. *Physica Scripta*, *95*(8), 085301.

Araz, A., Kavaz, E. & Durak, R. (2021). Neutron and photon shielding competences of aluminum open-cell foams filled with different epoxy mixtures: An experimental study. *Radiation Physics and Chemistry*, 182, 109382.

Banerjee, B., Bhattacharjee, Y. & Bose, S. (2019). Lightweight Epoxy-Based Composites for EMI Shielding Applications. *JOM*, 49, 1702–1720.

Canel, A., Korkut, H. & Korkut, T. (2019). Improving neutron and gamma flexible shielding by adding medium-heavy metal powder to epoxy based composite materials. *Radiation Physics and Chemistry*, 158, 13-16.

Castley, D., Goodwin, C. & Liu, J. (2019). Computational and experimental comparison of boron carbide, gadolinium oxide, samarium oxide, and graphene platelets as additives for a neutron shield. *Radiation Physics and Chemistry*, 165, 108435.

Crawley, A. (1974). Densities of liquid metals and alloys. *International Metallurgical Reviews*, *19*(1), 32-48.

Dong, M.G., Tishkevich, D.I., Hanfi, M.Y., Semenishchev, V.S., Sayyed, M.I., Zhou, S.Y., …, & Trukhanov, A.V. (2022). WCu composites fabrication and experimental study of the shielding efficiency against ionizing radiation. *Radiation Physics and Chemistry*, 200, 110175.

El-Fiki, S., El Kameesy, S.U., El. Nashar, D.E., Abou-Leila, M.A., El-Mansy, M.K. & Ahmed, M. (2015). Influence of bismuth contents on mechanical and gamma ray attenuation properties of silicone rubber composite. *IJAR, 3*(6), *1035*-1039.

El-Khatib, A.M., Abbas, M.I., Elzaher, M.A., Badawi, M.S., Alabsy, M.T., Alharshan, G.A. & Aloraini, D.A. (2019) Gamma Attenuation Coefficients of Nano Cadmium Oxide/High density Polyethylene Composites. *Scientific Reports*, 9, 16012.

Elsafi, M., Almousa, N., Al-Harbi, N., Almutiri, M.N., Yasmin, S. & Sayyed, M.I. (2023). Ecofriendly and radiation shielding properties of newly developed epoxy with waste marble and $WO_3$ nanoparticles. *Journal of Materials Research and Technology*, 22, 269-277.

Higgins, M.M.M., Radcliffe, N.A., Toro-González, M. & Rojas, J. (2019). Gamma ray attenuation of hafnium dioxide- and tungsten trioxide-epoxy resin composites. *JRNC*, 322, 707-716.

Hou, Y., Li, M., Gu, Y., Yang, Z., Li, R. & Zhang, Z. (2017). Gamma ray shielding property of tungsten powder modified continuous basalt fiber reinforced epoxy matrix composites. *Polymer Composites*, 39, 2106-2115.

İrim, Ş.G., Wis, A.A., Keskin, M.A., Baykara, O., Ozkoc, G., Avcı, A., Doğru, M. & Karakoç, M. (2018). Physical, mechanical and neutron shielding properties of h-BN/$Gd_2O_3$/ HDPE ternary nanocomposites. *Radiation Physics and Chemistry*, 144, 434-443.

Karabul, Y., İçelli, O. (2021). The assessment of usage of epoxy based micro and nano-structured composites enriched with $Bi_2O_3$ and $WO_3$ particles for radiation shielding. *Results in Physics*, 26, 104423.

Khattari, Z.Y., Al-Buriahi, M.S. (2022). Monte Carlo simulations and Phy-X/PSD study of radiation shielding effectiveness and elastic properties of barium zinc aluminoborosilicate glasses. *Radiation Physics and Chemistry*, 195, 110091.

Kim, J., Seo, D., Lee, B.C., Seo, Y.S. & Miller, W.H. (2014). Nano-W Dispersed Gamma Radiation Shielding Materials. *Advanced Engineering Materials, 16*(9), 1083-1089.

Kozlovskiy, A.L. Kenzhina, I.E., Zdorovets, M.V., Saiymova, M., Tishkevich, D.I., Trukhanov, S.V. & Trukhanov, A.V. (2019). Synthesis, phase composition and structural and conductive properties of ferroelectric microparticles based on $ATiO_x$ (A = Ba, Ca, Sr). *Ceramics International*, 45, 17236-17242.

Lacomme, E., Sayyed, M.I., Sidek, H.A.A., Matori, K.A. & Zaid, M.H.M. (2021). Effect of bismuth and lithium substitution on radiation shielding properties of zinc borate glass system using Phy-X/PSD simulation. *Results in Physics*, 20, 103768.

Li, R., Gu, Y., Zhang, G., Yang, Z., Li, M. & Zhang, Z. (2017). Radiation shielding property of structural polymer composite: Continuous basalt fiber reinforced epoxy matrix composite containing erbium oxide. *Composites Science and Technology*, 143, 67-74.

Li, X., Wu, J., Tang, C., He, Z., Yuan, P., Sun, Y., Lau, W.-M., Zhang, K., Mei, J. & Huang, Y. (2019). High temperature resistant polyimide/boron carbide composites for neutron radiation shielding. *Composites Part B: Engineering*, 159, 355-361.

Liu, Y., Liu, B., Gu, Y. & Wang, S. (2022). Gamma radiation shielding property of continuous fiber reinforced epoxy matrix composite containing functional filler using Monte Carlo simulation. *Nuclear Materials and Energy*, 33, 101246.

Lozitsky, O.V., Vovchenko, L.L., Matzui, L.Y., Oliynyk, V.V. & Zagorodnii, V.V. (2020). Microwave properties of epoxy composites with mixed fller carbon nanotubes/$BaTiO_3$. *Applied Nanoscience*, 10, 2759–2767.

Muthamma, M.V., Bubbly, S.G. & Gudennavar, S.B. (2019). Attenuation properties of epoxy-$Ta_2O_5$ and epoxy-$Ta_2O_5$- $Bi_2O_3$ composites at γ-ray energies 59.54 and 662 keV. *Journal of Applied Polymer Science*, 137, 49366.

Pavlenko, V.I., Cherkashina, N.I. & Yastrebinsky, R.N. (2019). Synthesis and radiation shielding properties of polyimide/$Bi_2O_3$ composites. *Heliyon, 5*, e01703.

Pitchan, M.K., Bhowmik, S., Balachandran, M. & Abraham, M. (2017). Process Optimization of Functionalized MWCNT/Polyetherimide Nanocomposites for Aerospace Application. *Materials & Design*, 127, 193-203.

Prabhu, S., Bubbly, S.G. & Gudennavar, S.B. (2021). Thermal, mechanical and γ-ray shielding properties of micro- and nano-Ta2O5 loaded DGEBA epoxy resin composites. *Journal of Applied Polymer Science*, 138, 51289.

Rohini, R., Bose, S. (2019). Electrodeposited carbon fiber and epoxy based sandwich architectures suppress electromagnetic radiation by absorption. *Composites Part B: Engineering*, 161, 578-585.

Saba, N., Jawaid, M., Alothman, Y.O., Paridah, M.T. & Hassan, A. (2015). Recent advances in epoxy resin, natural fiber-reinforced epoxy composites and their applications. *Journal of Reinforced Plastics and Composites*, *35*(6), 447-470.

Sahin, N., Bozkurt, M., Karabul, Y., Kiliç, M. & Ozdemir, Z.G. (2021). Low cost radiation shielding material for low energy radiation applications: Epoxy/Yahyali Stone composites. *Progress in Nuclear Energy*, 135, 103703.

Saiyad, M. & Devashrayee, N.M. (2021). Lifetime estimation of epoxy based composite materials on irradiating with gamma radiation for shielding applications. *Polymer Testing*, 93, 106929.

Şakar, E., Özpolat Ö.F., Alım, B., Sayyed, M.I. & Kurudirek, M. (2020). Phy-X / PSD: Development of a user friendly online software for calculation of parameters relevant to radiation shielding and dosimetry. *Radiation Physics and Chemistry*, 166, 108496.

Saleem, R.A.A., Abdelal, N., Alsabbagh, A., Al-Jarrah, M. & Al-Jawarneh, F. (2021). Radiation Shielding of Fiber Reinforced Polymer Composites Incorporating Lead Nanoparticles — An Empirical Approach. *Polymers*, 13, 3699.

Sayyed, M.I. (2016). Investigation of shielding parameters for smart polymers. *Chinese Journal of Physics*, 54, 408-415.

Sayyed, M.I., Albarzan, B., Almuqrin, A.H., El-Khatib, A.M., Kumar, A., Tishkevich, D.I., Trukhanov, A.V. & Elsafi, M. (2021a). Experimental and theoretical study of radiation shielding features of $CaO$-$K_2O$-$Na_2O$-$P_2O_5$ glass systems. *Materials*, *14*(14), 3772.

Sayyed, M.I., Al-Hadeethi, Y., AlShammari, M.M., Ahmed, M., Al-Heniti, S.H. & Rammah, Y.S. (2021b). Physical, optical and gamma radiation shielding competence of newly boro-tellurite based glasses: $TeO_2$–$B_2O_3$–$ZnO$–$Li_2O_3$–$Bi_2O_3$. *Ceram. Int.*, *47*(1), 611-618.

Sayyed, M.I., Dwaikat, N., Mhareb, M.H.A., D'Souza, A.N., Almousa, N., Alajerami, Y.S.M., Almasoud, F., Naseer, K.A., Kamath, S.D., Khandaker, M.U., Osman, H. & Alamri, S. (2022). Effect of $TeO_2$ addition on the gamma radiation shielding competence and mechanical properties of boro-tellurite glass: an experimental approach. *Journal of Materials Research and Technology*, 18, 1017-1027.

Shang, Y., Yang, G., Su, F., Feng, Y., Ji, Y., Liu, D., Yin, R., Liu, C. & Shen, C. (2020). Multilayer polyethylene/ hexagonal boron nitride composites showing high neutron shielding efficiency and thermal conductivity. *Composites Communications*, 19, 147-153.

Shin, J.W., Lee, J.W., Yu, S., Baek, B.K., Hong, J.P., Seo, Y., Kim, W.N., Hong, S.M. & Koo, S.M. (2014). Polyethylene/boron-containing composites for radiation shielding. *Thermochimica Acta*, 585, 5-9.

Singh, J.P., Singh, J., Kaur, P., Kaur, S., Arora, D., Kaur, R., Kaur, K. & Singh, D.P. (2020). Analysis of enhancement in gamma ray shielding proficiency by adding $WO_3$ in $Al_2O_3$-

$PbO\text{-}B_2O_3$ glasses using Phy-X/PSD. *Journal of Materials Research and Technology*, *9*(6), 14425-14442.

Thibeault, S.A., Kang, J.H., Sauti, G. & Park, C. (2015). Nanomaterials for radiation shielding. *MRS Bulletin*, 40, 836-841.

Tishkevich, D.I., Grabchikov, S.S., Lastovskii, S.B., Trukhanov, S.V., Vasin, D.S., Zubar, T.I., …, & Trukhanov A.V. (2019). Function composites materials for shielding applications: Correlation between phase separation and attenuation properties. *Journal of Alloys and Compounds*, 771, 238-245.

Tishkevich, D.I., Grabchikov, S.S., Lastovskii, S.B., Trukhanov, S.V., Zubar, T.I., Vasin, D.S. & Trukhanov, A.V. (2018 a). Correlation of the synthesis conditions and microstructure for Bi-based electron shields production. *Journal of Alloys and Compounds*, 749, 1036-1042.

Tishkevich, D.I., Grabchikov, S.S., Lastovskii, S.B., Trukhanov, S.V., Zubar, T.I., Vasin, D.S., …, & Zdorovets, M.V. (2018 b). Effect of the Synthesis Conditions and Microstructure for Highly Effective Electron Shields Production Based on Bi Coatings. *ACS Applied Energy Materials*, *1*(4), 1695-1702.

Tishkevich, D.I., Vorobjova, A.I. & Trukhanov, A.V. (2020a). Thermal stability of nano-crystalline nickel electrodeposited into porous alumina. *Solid State Phenomena*, 299, 281-286.

Tishkevich, D.I., Vorobjova, A.I. & Vinnik, D.A. (2020b). Formation and corrosion behavior of Nickel/Alumina nanocomposites. *Solid State Phenomena*, 299, 100-106.

Tishkevich, D.I., Zubar, T.I., Zhaludkevich, A.L., Razanau, I.U., Vershinina, T.N., Bondaruk, …, & Trukhanov, A.V. (2022). Isostatic hot pressed W–Cu composites with nanosized grain boundaries: microstructure, structure and radiation shielding efficiency against gamma rays. *Journal of Nanomaterials*, 12, 1642.

Trukhanov, A.V., Tishkevich, D.I., Podgornaya, S.V., Kaniukov, E., Darwish, M.A., Zubar, T.I., …, & Trukhanov, S.V. (2022). Impact of the nanocarbon on magnetic and electrodynamic properties of the ferrite/polymer composites. *Journal of Nanomaterials*, 12, 868.

Verdipoor, K., Alemi, A. & Mesbahi, A. (2018). Photon mass attenuation coefficients of a silicon resin loaded with $WO_3$, PbO, and $Bi_2O_3$ micro and nano-particles for radiation shielding. *Radiation Physics and Chemistry*, 147, 85-90.

Vorobjova, A.I., Shimanovich, D.L., Sycheva, O.A., Ezovitova, T.I., Tishkevich, D.I. & Trykhanov, A.V. (2019). Studying the thermodynamic properties of composite magnetic material based on anodic alumina. *Russian Microelectronics*, *48*(2), 107-118.

Wani, A.L., Ara, A. & Usmani, J.A. (2015). Lead toxicity: a review. *Interdisciplinary Toxicology*, *8*(2), 55-64.

Wu, Z.X., Li, J.W., Huang, C.J., Huang, R.J. & Li, L.F. (2013). Effect of gamma irradiation on the mechanical behavior, thermal properties and structure of epoxy/glass-fiber composite. *Journal of Nuclear Materials*, 441, 67-72.

Yılmaz, S.N., Akbay, İ.K. & Özdemir, T. (2021). A metal-ceramic-rubber composite for hybrid gamma and neutron radiation shielding. *Radiation Physics and Chemistry*, 180, 109316.

Yu, L., Yap, P.L., Santos, A., Tran, D. & Losic, D. (2021). Lightweight bismuth titanate ($Bi_4Ti_3O_{12}$) nanoparticle-epoxy composite for advanced lead-free X-ray radiation shielding. *ACS Applied Nano Materials*, 4, 7471-7478.